Heliyon Volume Number update (2021) e05949

Contents lists available at ScienceDirect

Heliyon

journal homepage: www.cell.com/heliyon

Research article

Electrochemical corrosion behavior of copper in graphene-based thermal fluid with different surfactants

Adeola O. Borode [a,*], Noor A. Ahmed [a], Peter A. Olubambi [b]

[a] Department of Mechanical Engineering Science, University of Johannesburg, Johannesburg, South Africa
[b] Department of Metallurgy, University of Johannesburg, Johannesburg, South Africa

ARTICLE INFO

Keywords:
Graphene
Nanofluid
Potentiodynamic polarization
Corrosion
Copper

ABSTRACT

This study investigates the effect of different surfactant-dispersed graphene nanofluid on the electrochemical behavior of copper. This study was achieved by measuring the open circuit potential and potentiodynamic polarization of copper in the nanofluids at room temperature. The test media includes surfactant-free graphene nanofluid and graphene nanofluid dispersed using four different surfactants, which are sodium dodecyl sulfate, sodium dodecylbenzene sulfonate, Gum Arabic, and Tween 80. The surface characterization and elemental composition of the copper sample before and after the corrosion tests were determined using a scanning electron microscope coupled with energy-dispersive X-ray spectroscopy. The phase formation after corrosion was also evaluated by measuring X-ray diffraction. The quantity of copper dissolved in the test media was evaluated using an inductively coupled plasma mass spectrometry (ICP-MS). The open-circuit potential measurements revealed that the current free corrosion potential of copper in the different surfactant-aided graphene nanofluids are different. The electrochemical corrosion potential, Tafel slopes, and corrosion rates revealed the better corrosion performance of copper in the nanofluid of different surfactants in the increasing order GA, SDS, Tween 80, and SDBS. Copper in GA-based graphene nanofluid was found to have the lowest corrosion rate while that of SDBS has the highest corrosion rate. However, the ICP-MS result revealed a discrepancy in the corrosion behavior and quantity of copper dissolved in the different test media. This could be attributed to the dissimilar dissolution-redeposition rate of copper in different media.

1. Introduction

Over the past few years, nanofluids, which is a nanoparticle-based thermal fluid, have been greatly investigated for heat transfer applications. This is mostly due to nanofluids' enhanced thermal properties compared to conventional fluids such as water, ethylene glycol, engine oil, etc. These enhanced properties ensure that nanofluid can be applied mainly in process cooling and heating, electronic cooling, cooling of heavy-duty vehicles or machinery, solar collectors, and other numerous heat exchangers. Numerous articles have been published on nanofluids' heat transfer application [1, 2, 3, 4, 5].

Nanofluids are mostly prepared by a two-step approach, which involves the dispersion of dry nanomaterials into conventional fluids [1]. However, few studies reported the use of one-step simultaneous synthesis of nanomaterials and dispersion in conventional fluids. This one-step approach results in a better stable nanofluid production than the two-step approach, but it is more costly [6]. Numerous nanomaterials have also been used for preparing nanofluids. They include metallic nanomaterials (Cu, Au, Zn, etc.) [7], metal oxides nanomaterials (CuO, Fe_2O_3, Al_2O_3, TiO_2, SiO_2, MnO_2, etc.) [8] and carbon nanomaterials (Carbon nanotubes, graphene, nano-diamond, fullerenes, etc.) [9]. Amongst the nanomaterials, carbon nanomaterials, most especially graphene, have been extensively reported to have a very high thermal conductivity [2]. This indicates that they can be used to prepare nanofluids with superior heat transfer performance. However, like other carbon nanomaterials such as carbon nanotubes (CNT), graphene is highly hydrophobic, which means they tend to agglomerate when suspended in conventional fluids [10, 11]. Thus, surfactants, which reduce surface tension, are mostly used to stably disperse graphene in conventional fluids with an ultrasonicator. Borode et al. [9] comprehensively reported on the application of various surfactants such as sodium dodecyl sulfate (SDS), sodium dodecylbenzene sulfonate (SDBS), Polyethylene sorbitol ester (also known as Tween 80), Gum Arabic (GA), Polyvinylpyrrolidone (PVP), Cetrimonium bromide (CTAB), Triton X-100,

* Corresponding author.
E-mail addresses: aborode@uj.ac.za, hadeyola2003@yahoo.com (A.O. Borode).

https://doi.org/10.1016/j.heliyon.2021.e05949
Received 28 October 2020; Received in revised form 2 December 2020; Accepted 7 January 2021

Table 1. Properties and details of Surfactants supplied by Sigma Aldrich.

Surfactant	Molecular Formula	Molecular Weight (g/mol)	Form	Product Number	CAS Number
SDS	$C_{12}H_{25}NaO_4S$	288.38	Powder	L4509	151-21-3
SDBS	$C_{18}H_{29}NaO_3S$	348.48	Powder	289957	25155-30-0
GA	-	-	Powder	G9752	9000-01-5
Tween 80	-	-	Viscous Liquid	P1754	9005-65-6

Table 2. Description and details of graphene nanoplatelets supplied by Sigma Aldrich.

Nanomaterial	Particle Size (μm)	Surface area (m^2/g)	Molecular Weight (g/mol)	Average Thickness (nm)	Form	Product Number	CAS Number
GNP	5	50–80	12.01	15	Powder	900409	7782-42-5

Table 3. Composition of UNS C11000 copper alloy.

Element	Cu	Si	Fe	Pb	P	Mn
Composition (%)	99.9	0.008	0.002	0.002	0.03	0.001

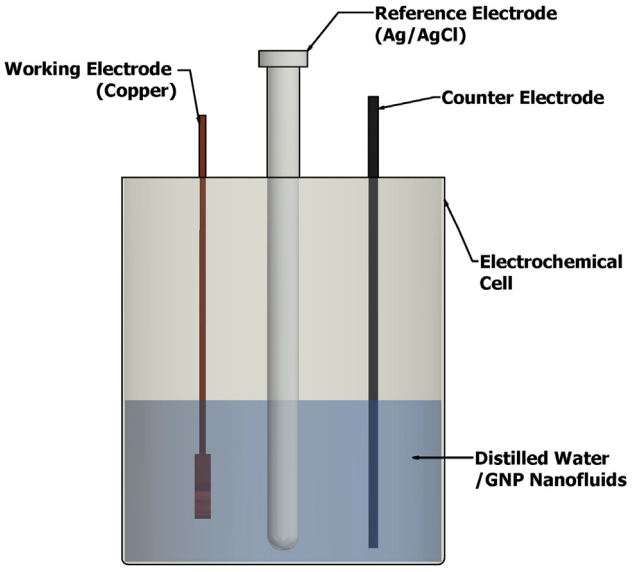

Figure 1. Electrochemical corrosion test set-up.

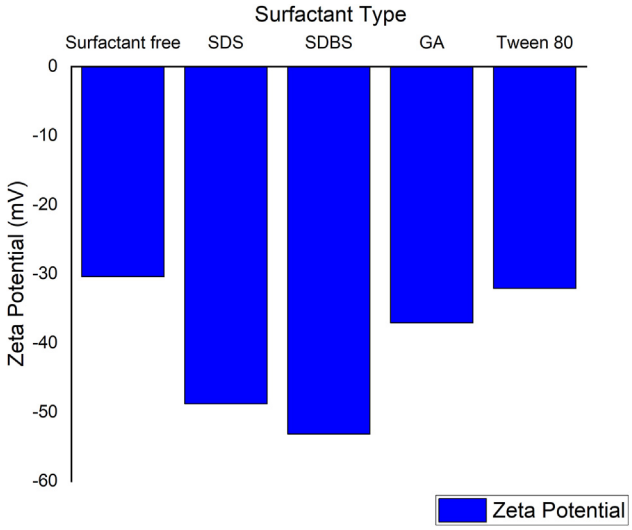

Figure 2. Zeta potential of the graphene nanofluids prepared with the different surfactants.

etc. for preparing a stable carbon-based nanofluid. They observed that surfactant-dispersed nanofluids remained stable for at least two weeks to six months.

Also, the thermophysical properties of graphene-based nanofluids have been investigated by numerous authors. Sadeghinezhad et al. [12] reported a thermal conductivity increase of 7.96–25% for 0.025–0.1 wt% graphene nanoplatelet (GNP) nanofluid. Mehrali et al. [13] reported a thermal conductivity augmentation of 27.64% for nanofluid prepared with 0.1 wt% GNP of 750 m^2/g specific surface area (SSA). In a review study of the thermal application of carbon-based nanofluid, Borode et al. [2] reported an improved thermal efficiency of up to 93.2% and 90.7% for flat plate solar collector [14] and evacuated tube solar collector [15] using nanofluid with graphene loading of 0.005 wt% and 0.1wt vol% respectively.

Despite the availability of numerous studies on the stability, thermophysical properties, and heat transfer efficiency of graphene nanofluids, little to no studies exist on the nanofluid's corrosion and erosion effects on heat exchanger materials. Nonetheless, the study of corrosion effect is more paramount than that of erosion. This is because the material loss has been reported to be majorly through the chemical effect (corrosion) than the mechanical effect (erosion) [16]. Based on our knowledge, no study has been made on the corrosion effect of graphene nanofluids. However, some studies have been made on other types of nanofluid. Rashidi et al. [17] evaluated the corrosion rate of carbon steel in MWCNT nanofluid by measuring the potentiodynamic polarization. The corrosion behavior of SDS and SDBS-dispersed MWCNT nanofluids was compared to that of functionalized MWCNT nanofluid. They observed a corrosion rate of 3.3402 mpy and 1.643 mpy for SDBS and SDS-dispersed nanofluid, which is higher than that of distilled water. However, the addition of functionalized MWCNT was found to reduce the corrosion rate of distilled water.

Ismail et al. [18] studied the corrosion rates of copper, aluminum, and stainless steel in GA-dispersed CNT nanofluids. They reported that copper has the least corrosion rate, followed by stainless steel, with aluminum having the highest corrosion rate. Corrosion rates of all the metal were also found to increase with temperature. The corrosion rates in all the nanofluids were reported to be lower than in water and ethylene glycol. This was attributed to the corrosion inhibitive tendency of GA. Wu et al. [19] investigated the corrosive behavior of brass in TiO_2 nanofluids with SDBS dispersant. They observed that the addition of TiO_2 in base

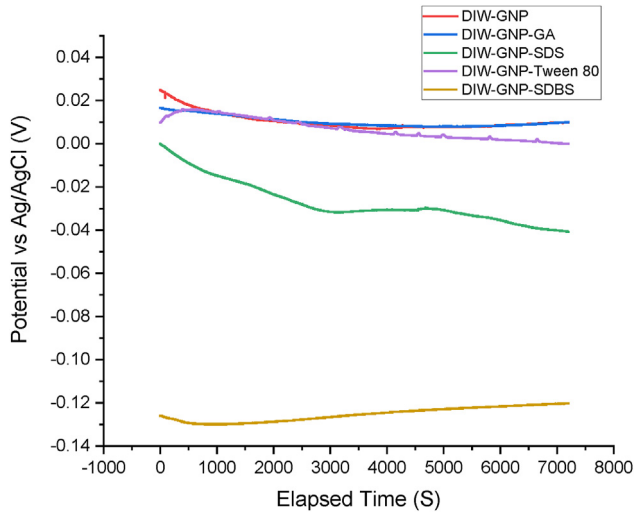

Figure 3. Open Circuit Potential of the copper in different GNP nanofluids.

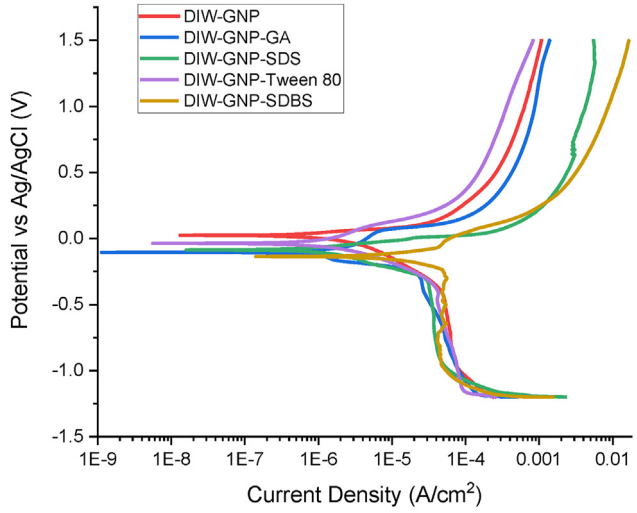

Figure 4. Polarization curve of copper in the distilled water and the different GNP nanofluids.

simulated cooling water leads to an increase in brass corrosion, while the addition of SDBS effectively inhibits corrosion. Yuan et al. [20] also affirm the corrosion inhibitive behavior of SDBS surfactant. They investigated the corrosion behavior of brass in Al_2O_3-simulated cooling water-based nanofluid. The nanofluid was prepared with and without SDBS dispersant. They found that Al_2O_3 and SDBS synergized to hinder corrosion of brass in nanofluid by promoting the formation of a protective film on the brass surface.

It was observed that the previous studies reported conflicting results as regards the inhibiting properties of surfactants. Some researchers reported

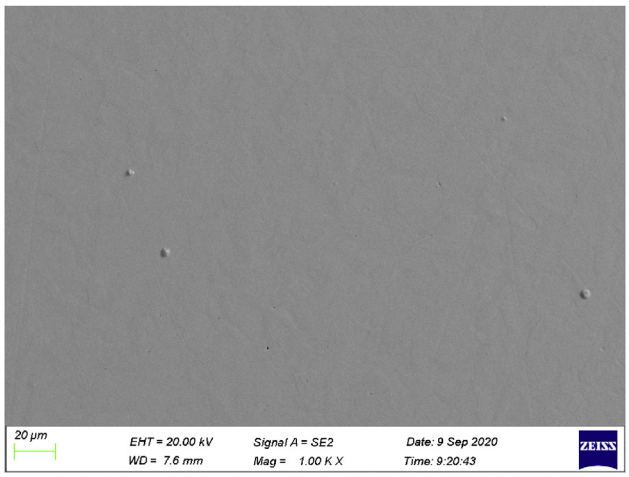

Figure 5. SEM micrograph of the bare copper sample before corrosion.

that surfactants are inhibitors, which prevent or reduces corrosion [18, 20, 21], while some other studies revealed that surfactants increase corrosion of metal [17, 22]. This indicates that more studies need to be conducted to effectively evaluate the effect of surfactants on the corrosive behavior of metals in nanofluids. Copper alloy is a major metal used as thermal exchange materials in heat exchangers or solar collectors. This study will focus on copper primarily because it is commercially a material of choice for solar collectors and heat exchangers. This is because it has high heat and electricity conductivity coupled with its ductility and workability. Despite the reasonable corrosion resistance attribute of copper, numerous studies have reported its susceptibility to corrosion in a solar water heating system [23]. Thus, research studies on the corrosion effect of graphene nanofluid on copper alloy are important from an economical and safety perspective towards heat transfer application of the nanofluid.

Corrosion is an irreversible chemical reaction of a metallic material with its environment, which leads to the wastage or degradation of metal [24]. This indicates that corrosion could cause failure, reduce efficiency, and increase the maintenance cost of thermal equipment. Thus, due to the exceptional thermal properties of graphene nanofluids, this study aims to study its corrosion effect on copper. First, graphene-based nanofluids were prepared with and without surfactants, which include SDS, SDBS, GA, and Tween 80. The stability of these nanofluids was evaluated. Thirdly, the effects of different surfactants on the corrosion behavior of copper heat exchange material were investigated using open circuit potential, potentiodynamic polarization, scanning electron microscope, and X-ray diffraction.

2. Materials and methods

2.1. Materials and preparation of nanofluids

Graphene nanoplatelets, deionized water, and four different surfactants were used in the preparation of the nanofluid. The surfactants used include SDS, SDBS, GA, and Tween 80. All the surfactants and GNP were

Table 4. Corrosion potentiodynamic properties of copper examined in different Nanofluids at room temperature.

Test Media	E_{corr} (mV)	β_a (mV/dec)	β_c (mV/dec)	j_{corr} (µA/cm^2)	Inhibition Efficiency
DIW-GNP	26.13	88.99	292.28	0.1669	-
DIW-GNP-GA	-106.95	193.00	130.25	0.0951	42.99%
DIW-GNP-SDS	-85.23	102.76	191.87	0.1236	25.93%
DIW-GNP-Tween 80	-36.28	232.62	206.44	0.1430	14.35%
DIW-GNP-SDBS	-136.13	145.92	172.45	1.1504	-

$\boldsymbol{\beta_a}$ = Anodic Beta, $\boldsymbol{\beta_c}$ = Cathodic Beta, j_{corr} = Current density.

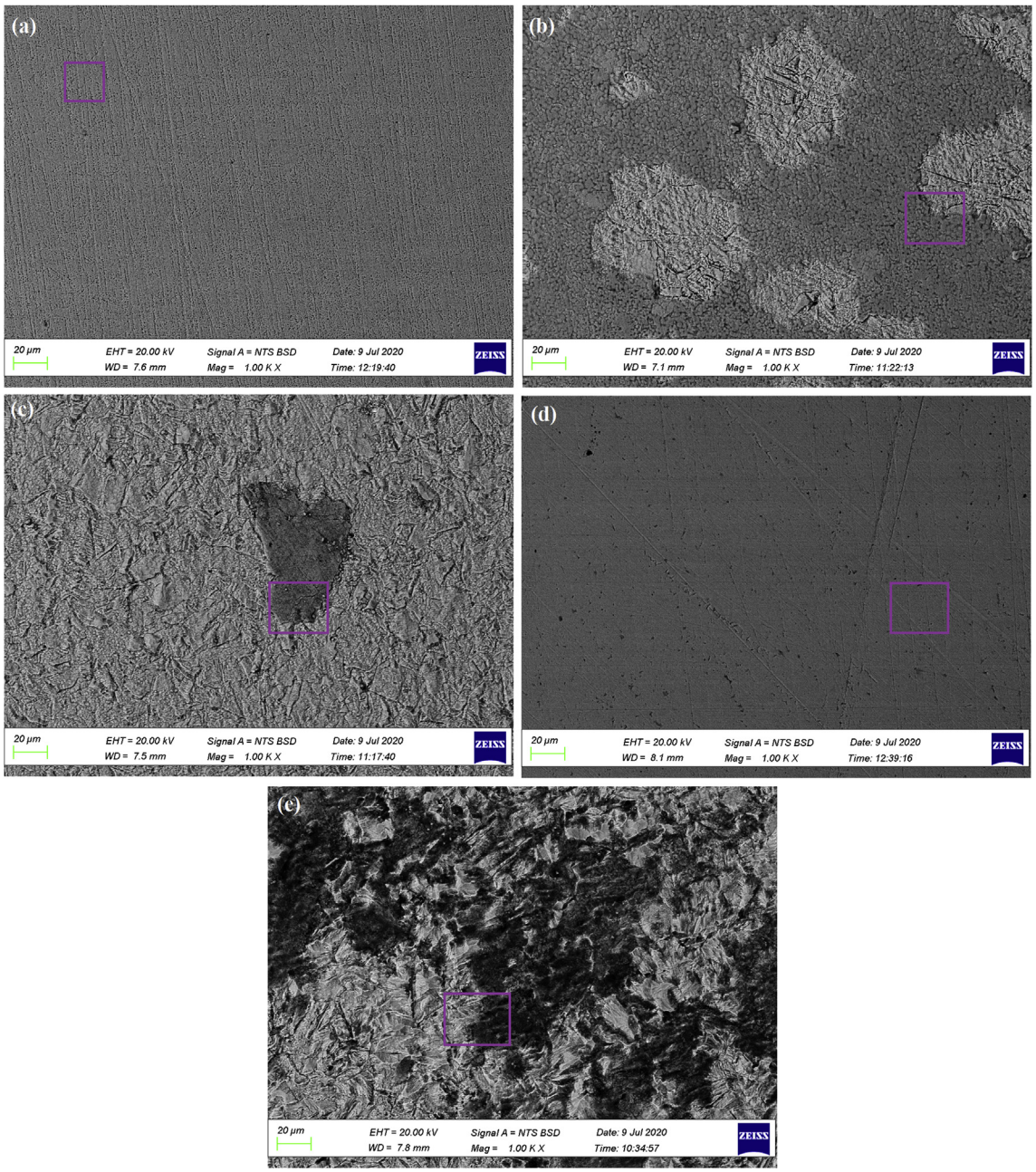

Figure 6. SEM micrograph of the copper alloy surface after polarization test in graphene nanofluid with (a) no surfactant (b) GA (c) SDS (d) Tween 80 (e) SDBS.

purchased from Sigma-Aldrich Chemie GmbH, Germany. The GNP has a particle size of 5 µm and a specific surface area of 80 m^2/g. The properties of the materials mentioned above are listed in Table 1 and Table 2. The nanofluids were prepared using a two-step method of preparation. A solution was first prepared by dispersing the surfactant into deionized water with a magnetic stirrer. This was followed by the addition of GNP at a surfactant/nanomaterial ratio of 1:1. The solution was further ultrasonicated for 30 min to ensure the stability of the nanofluids. This method was repeated to prepare nanofluid with the different surfactants and without surfactant. Further, the stability of the prepared nanofluids was evaluated using a zeta potential analyzer. The zeta potential value was measured using Malvern Zetasizer Nano ZS.

Cylindrical copper electrodes, which were cold mounted using resin, with an exposed surface area of 12.57 cm^2, were used for the electrochemical corrosion test. The cylindrical working electrode specimen with dimension φ20 mm × 5 mm were cut from UNS C11000 (CDA110) copper alloy electrode rod. The elemental composition of the copper alloy is listed in Table 3. Before the corrosion tests, all the cylindrical samples were sequentially ground and polished to 0.2 µm surface finish.

2.2. Electrochemical measurements

Electrochemical techniques were employed to evaluate the effects of surfactants on the corrosion behavior of copper in graphene nanofluids. These techniques include open circuit potential (OCP) measurement and potentiodynamic polarization. All the electrochemical corrosion tests were performed using Versa-STAT 4 standard electrochemical workstation at room temperature. As presented in Figure 1, the tests were done with a three-electrode electrochemical cell set-up, which comprises a silver-silver chloride reference electrode, a platinum rod counter electrode, and the cylindrical copper specimen as the working electrode.

Before performing the polarization test, OCP was performed on the copper specimens in all the nanofluids (with and without surfactants) for

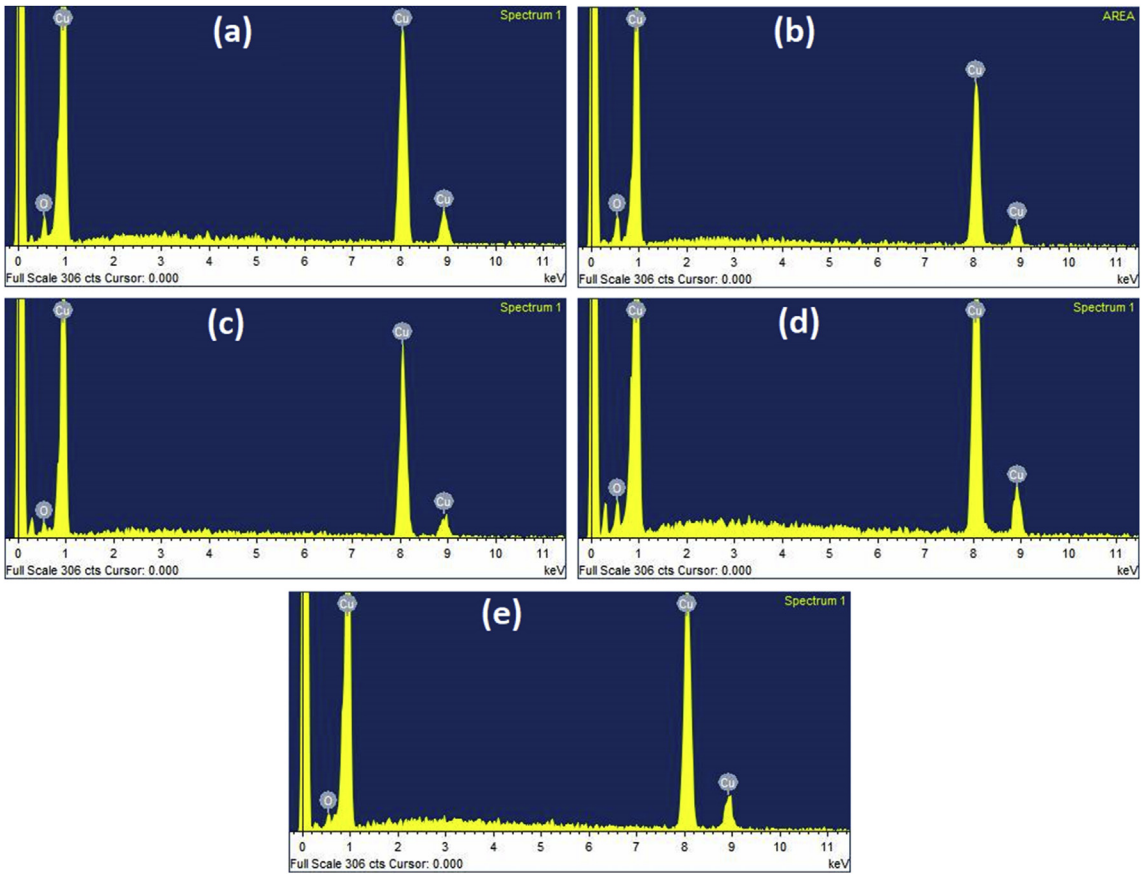

Figure 7. EDS Spectrum of the marked copper alloy surface after polarization test in graphene nanofluid with (a) no surfactant (b) GA (c) SDS (d) Tween 80 (e) SDBS.

7200s to establish current-free potential (E_{OCP}) with respect to the reference electrode. The potentiodynamic polarization measurements were conducted using a scan rate of 0.1667 mV/s at a potential between -1.2 V to 1.5 V. Electrochemical parameters such as corrosion rate, Tafel slopes, $E_{corr,}$ and I_{corr} were analyzed using the VersaStudio and CorrView software.

2.3. Surface characterization

The microstructural features of the corroded and uncorroded copper surface were observed using an optical microscope. For in-depth surface analysis, a high-resolution Zeiss Sigma Field Emission Scanning Electron Microscope (FESEM) ® fitted with an Oxford energy dispersive X-ray (EDS) detector was employed to analyze the surface morphology and elemental composition of the copper specimens. The phase characterization of the corroded samples' surface was evaluated by measuring the X-ray diffraction patterns using a PANalytical X'Pert PRO X-Ray Diffractometer. The obtained XRD patterns were further analyzed using PANalytical HighScore software (version 3.0.5).

Table 5. Atomic composition of the elements present on the copper surface immersed in different media.

Test Media	% Atom	
	Cu	O
DIW-GNP	83.66	16.34
DIW-GNP-GA	75.94	24.06
DIW-GNP-SDS	90.07	9.93
DIW-GNP-Tween 80	85.47	14.53
DIW-GNP-SDBS	91.43	8.57

2.4. Analysis of the corrosion solutions

After the polarization tests, a quadrupole-based PerkinElmer NexION 300D Inductively coupled plasma mass spectrometry (ICP-MS) was used to analyze the concentration of copper dissolved in the different test media. The test media were first centrifuged to separate the graphene from the fluids to prevent interference during analysis. The obtained fluid was then filtered and diluted (1:10) with 1% nitric acid (HNO_3) to achieve stability. The isotope Cu^{63} was subsequently measured.

3. Results and discussions

3.1. Stability of the graphene nanofluids

Stability is a major factor, which is necessary to ensure the long-term thermal application of graphene nanofluids. Hence, the stability of the different nanofluids was studied using Zeta potential analysis. Zeta potential analysis is the measurement of the potential difference between the dispersing fluid and the stationary surface of the fluid attached to the suspended nanomaterials [25]. Zeta potential value is an indicator of the repulsive force between the nanomaterial and the base fluid. A nanofluid with a high absolute zeta potential, which is more or equal to 30, is deemed stable, while a low absolute zeta potential of less than 30 mV indicates poor stability.

Zeta potentials of all the graphene nanofluids were measured at room temperature of 25 °C to obtain an accurate measure of stability. As shown in Figure 2, all the nanofluids show good stability. SDBS was observed to exhibit the highest stability with a zeta potential value of -53.2 mV. This was followed by SDS, GA, and Tween 80 with zeta potential values of -48.8 mV, -37.1 mV, and -32.1 mV. These zeta potential values show that all the surfactants effectively contribute an improvement to the stability

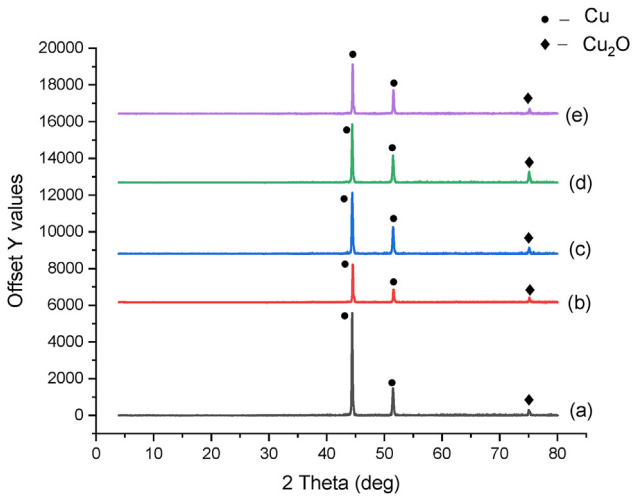

Figure 8. XRD results of the copper surface after OCP and potentiodynamic polarization test in graphene nanofluid with (a) no surfactant (b) GA (c) SDS (d) Tween 80 (e) SDBS.

of graphene nanofluids. This is evident in the zeta potential value of the surfactant-free graphene nanofluid, which is the lowest (-30 mV). The value of all the zeta potential value indicates that the surface of the nanomaterials is negatively charged. This is because SDS and SDBS are anionic surfactants while GA and Tween 80 are non-ionic surfactants, which stabilizes due to steric repulsions. The nanofluids' stability was achieved due to the adsorption of the different surfactants onto the GNP's surface through van der Waals forces, which brings about an increase in the electrostatic repulsion between the GNP particles. Thus, higher surfactant adsorption to the nanomaterial surface results in an increased electrostatic repulsion between the nanomaterials and a more negative zeta potential value, which indicates higher stability. This shows that SDBS has a higher tendency to adsorb to GNP's surface than the other surfactants.

3.2. Open circuit potential and potentiodynamic polarization

The potentiodynamic polarization measurement was performed for copper alloy in different graphene nanofluids dispersed with or without surfactant. Figure 3 and Figure 4 shows the open circuit potential and potentiodynamic polarization curves of the copper alloy in different nanofluid, respectively. The open-circuit potential measurement was done for 2 h before the corrosion test. Corrosion properties such as corrosion potential (E_{corr}), current density (j_{corr}), anodic (β_a), and cathodic (β_c) Tafel slopes were obtained by fitting the polarization curves (Figure 4) as presented in Table 4. E_{corr} denotes the mixed potential at which the anodic dissolution of copper equals the cathodic reaction and no net current flowing in or out of the copper electrode. Further, j_{corr} indicates the dissolution current per unit area of copper at E_{corr}.

Figure 3 shows the changes in the open circuit potential (E_{OCP}) of copper in the different nanofluids for 7200s. These changes indicate some of the corrosion behavior of the copper alloy. It can be observed that the stable E_{OCP} value of copper in DIW-GNP-SDBS is more negative than in other nanofluids. This shows that the copper alloy has a very high tendency to corrode in the presence of SDBS surfactant than other surfactants. Also, the addition of SDS and Tween 80 caused a decrease in the stable E_{OCP} of copper in DIW-GNP nanofluid, while the addition of GA seems to have little to no effect on the E_{OCP}. This indicates that copper alloy's electrochemical activity is greater in DIW-GNP nanofluid with the addition of SDBS, followed by SDS and Tween 80 in comparison to GA.

From the Tafel fitting results (Table 4), it can be observed that the lowest current density (j_{corr}) of 0.0951 μA/cm^2 was reported for copper in DIW-GNP-GA while copper in DIW-GNP-SDBS has the highest j_{corr}, of 1.1504 μA/cm^2. Further, the j_{corr} of copper was found to reduce with the addition of GA, SDS, and Tween 80 to the DIW-GNP nanofluid, while it increases significantly with the addition of SDBS. The j_{corr} of copper was found to be 0.0951 μA/cm^2, 0.1236 μA/cm^2, and 0.1430 μA/cm^2 in DIW-GNP-GA, DIW-GNP-SDS, and DIW-GNP-Tween 80, respectively. This clearly shows that all the surfactants except SDBS inhibit corrosion of copper in GNP nanofluids.

It is also pertinent to state that the various surfactants' addition also affects the Tafel slopes β_a and β_c. The addition of all the surfactants to DIW-GNP nanofluid causes a change in the values of β_a and β_c. This shows that most of the surfactants are mixed-type inhibitors. The addition of GA, SDS, and Tween 80 to DIW-GNP nanofluid produces an increase in the anodic Tafel slope β_a while also reducing the anodic current density j_{corr}. This indicates that these surfactants' adsorption inhibits the anodic dissolution of copper through the formation of a protective film on the copper surface. However, the addition of SDBS to the DIW-GNP nanofluid was observed to promote copper's anodic dissolution despite contributing an increase to the Tafel slope β_a. This is evidenced in its very high anodic current density j_{corr} and the more negative corrosion potential E_{corr} of copper. This could be attributed to the instability of the SDBS molecules adsorbed on the copper surface. This is because of the change in the anodic curve of the copper sample when the polarization potential increases above -70 mV (vs. ref.), which could be due to the desorption of the SDBS molecules from the copper surface. This corrosion-promoting behavior of SDBS was also reported in the study by Rashidi et al. [17].

The corrosion inhibition efficiency of the surfactants was calculated using the formula in Eq. (1).

$$Inhibition\ efficiency = \frac{j_0 - j_X}{j_0} \text{ x } 100\% \quad (1)$$

Where j_0 is the current density of copper in DIW-GNP nanofluid while j_x is the current density of copper in surfactant-based DIW-GNP nanofluids. The corrosion inhibition efficiency of the surfactant-based nanofluids is not ideal because the inhibition efficiency of GA, SDS, and Tween 80 are all less than 50%. The corrosion inhibition efficiency of copper in DIW-GNP-GA, DIW-GNP-SDS, and DIW-GNP-Tween 80 is approximately 43%, 26%, and 14%, respectively.

Table 6. ICP-MS results of the copper dissolved in the test media.

Test Media	^{63}Cu (μg/L)
DIW-GNP	19.634
DIW-GNP-GA	65.369
DIW-GNP-SDS	1200.722
DIW-GNP-Tween 80	13.038
DIW-GNP-SDBS	4604.899

3.3. Surface characterization

3.3.1. SEM and EDS analysis

Figure 5 shows the SEM micrograph of the bare copper electrode before corrosion. SEM images of the copper samples after the polarization test in the different test media are shown in Figure 6a-f. The corresponding images of the EDS analysis, which was done to assess the elemental composition on the corroded surface, are shown in Figure 7. As observed in Figure 6(a, b, d, and e) in comparison to Figure 5, the surface of the copper alloys was sparingly covered with a corrosion layer. The EDS analysis in Figure 7 shows that the major elemental composition on the different copper electrodes are Cu and O. This indicates the formation of a thin film protector of copper oxide on the electrodes' surface. This film reduces corrosion damages to the copper alloy. The atomic composition of the Cu and O for the copper electrode immersed in the different media are presented in Table 5. Some concentration of oxygen on the surface of the copper alloy, presented in Table 5, may be attributed

to the increase in the mass transfer of oxygen due to GNP. However, despite the presence of the Cu and O layer on the sample immersed in SDBS-based nanofluid (Figure 7c), a large area of black pits and damages were noticed on the copper alloy as shown in Figure 6c. It was also observed that the SDBS-based nanofluid offers little to no protection to the copper surface as loose corrosion products majorly cover the sample. This further confirms the potentiodynamic polarization results that SDBS promotes corrosion.

3.3.2. XRD analysis

Figure 8 shows the XRD results of the copper surface after the polarization test in the different test media. The main peaks are found at 44.51°, 51.61°, and 75.19° for all the test samples. All the peaks at 44.51° and 51.61° are ascribed to Cu. The diffraction peak of all the samples at 75.19° corresponds to cupric oxide (Cu_2O), which has the weakest peak intensity. This shows that the Copper oxide film formed on the copper surface is quite small. Thus, the anodic and cathodic reaction that might occur on the copper samples in the different test media during the polarization tests can be expressed as presented in Eqs. (2), (3), and (4) [26]:

Anodic reaction:

$$Cu \rightarrow Cu^{2+} + 2e \tag{2}$$

$$2Cu + H_2O \rightarrow Cu_2O + 2H^+ + 2e \tag{3}$$

Cathodic reaction:

$$O_2 + 2H_2O + 4e \rightarrow 4OH^- \tag{4}$$

3.4. ICP-MS analysis

After the electrochemical corrosion, the test media were analyzed using ICP-MS to evaluate the quantity of copper dissolved in the media. The results of this analysis are presented in Table 6. The analysis revealed that a significant amount of copper was dissolved in DIW-GNP-SDS and DIW-GNP-SDBS, which have the highest concentration. This high concentration of dissolved copper could be attributed to the sulfur composition of both SDS and SDBS. Numerous researchers have found sulfur-based media [27, 28] to attack copper and promote corrosion. However, despite the high amount of dissolved copper in DIW-GNP-SDS in comparison to that of other test media excluding DIW-GNP-SDBS, the copper sample in the SDS-based nanofluid exhibited a lower anodic current density as presented in Table 4. Further, this discrepancy between the anodic current density of copper and the amount of copper dissolved in the test media could be attributed to the different dissolution and redeposition tendency of copper in the various media. The Cu dissolution mechanism has been presented in Eq. (3), while the redeposition mechanism can be described as presented in Eqs. (5) and (6) [26].

$$Cu \rightarrow Cu^{2+} + 2e^- \tag{5}$$

$$Cu + Cu^{2+} + H_2O \rightarrow Cu_2O + 2H^+ \tag{6}$$

4. Conclusion

The corrosion behavior of copper was evaluated in different test media, which include surfactant-free graphene nanofluids and graphene nanofluids prepared with GA, SDS, SDBS, and Tween 80. The conclusions are as follow:

1. The dispersion of graphene in deionized water with surfactants reasonably improves the stability of DIW-GNP nanofluid. This is evident as all the surfactant-dispersed nanofluids exhibit an absolute zeta potential value that is greater than 30 mV. DIW-GNP-SDBS nanofluid exhibits the highest level of stability, followed by SDS, GA, and Tween 80-based nanofluid.
2. The addition of GA, SDS, or Tween 80 to GNP nanofluid inhibits the corrosion of copper in the nanofluid. However, SDBS surfactant was found to promote corrosion of copper, which is evident in its very high anodic current density of 1.1504 μA/cm^2. The inhibition efficiency of GA, SDS, and Tween 80 are 42.99%, 25.93%, and 14.35%, respectively.
3. The copper surface was protected by a thin film of cuprous oxide (Cu_2O). This was validated by the XRD and EDS results. This indicates that the corrosion mechanism occurs through two-electron oxidation reactions.
4. Finally, the study deduced that SDBS is very aggressive to the surface of the copper sample and result in the dissolution of a very high amount of copper in the nanofluid. On the other hand, the addition of GA, SDS, and Tween 80 reduces the anodic current density of copper.

Declarations

Author contribution statement

Adeola O. Borode: Conceived and designed the experiments; Performed the experiments; Analyzed and interpreted the data; Wrote the paper.

Noor A. Ahmed, Peter A. Olubambi: Conceived and designed the experiments; Contributed reagents, materials, analysis tools or data.

Funding statement

This work was supported by the National Research Foundation (NRF) of South Africa (Grant Number: 114650).

Data availability statement

Data will be made available on request.

Declaration of interests statement

The authors declare no conflict of interest.

Additional information

No additional information is available for this paper.

Acknowledgements

The authors appreciate the Centre for Nanoengineering and Tribocorrosion (CNT), University of Johannesburg, DFC Campus, for the use of their laboratory and equipment.

References

[1] A.O. Borode, N.A. Ahmed, P.A. Olubambi, A review of heat transfer application of carbon-based nanofluid in heat exchangers, Nano-Struct. Nano-Objects 20 (Oct. 2019) 100394.
[2] A. Borode, N. Ahmed, P. Olubambi, A review of solar collectors using carbon-based nanofluids, J. Clean. Prod. 241 (Dec. 2019) 118311.
[3] A.O. Borode, N.A. Ahmed, P.A. Olubambi, Application of carbon-based nanofluids in heat exchangers: current trends, J. Phys. Conf. Ser. 1378 (Dec. 2019), 032061.
[4] K. Farhana, et al., "Improvement in the performance of solar collectors with nanofluids — a state-of-the-art review, Nano-Struct. Nano-Objects 18 (Apr. 2019) 100276.
[5] V. Kumar, A.K. Tiwari, S.K. Ghosh, Application of nanofluids in plate heat exchanger: a review, Energy Convers. Manag. 105 (2015) 1017–1036.
[6] W. Yu, H. Xie, A review on nanofluids: preparation, stability mechanisms, and applications, J. Nanomater. 2012 (2012) 17.
[7] M. Raja, R. Vijayan, P. Dineshkumar, M. Venkatesan, Review on nanofluids characterization, heat transfer characteristics and applications, Renew. Sustain. Energy Rev. 64 (2016) 163–173.
[8] K.S. Suganthi, K.S. Rajan, Metal oxide nanofluids: review of formulation, thermo-physical properties, mechanisms, and heat transfer performance, Renew. Sustain. Energy Rev. 76 (2017) 226–255.

[9] A.O. Borode, N.A. Ahmed, P.A. Olubambi, Surfactant-aided dispersion of carbon nanomaterials in aqueous solution, Phys. Fluids 31 (7) (Jul. 2019), 071301.
[10] E.E. Tkalya, M. Ghislandi, G. de With, C.E. Koning, The use of surfactants for dispersing carbon nanotubes and graphene to make conductive nanocomposites, Curr. Opin. Colloid Interface Sci. 17 (4) (2012) 225–232.
[11] A.K. Rasheed, M. Khalid, W. Rashmi, T.C.S.M. Gupta, A. Chan, "Graphene based nanofluids and nanolubricants – review of recent developments, Renew. Sustain. Energy Rev. 63 (2016) 346–362.
[12] E. Sadeghinezhad, et al., An experimental and numerical investigation of heat transfer enhancement for graphene nanoplatelets nanofluids in turbulent flow conditions, Int. J. Heat Mass Tran. 81 (2015) 41–51.
[13] M.M. Mehrali, et al., Investigation of thermal conductivity and rheological properties of nanofluids containing graphene nanoplatelets, Nanoscale Res. Lett. 9 (1) (Jan. 2014) 15.
[14] M. Vakili, S.M. Hosseinalipour, S. Delfani, S. Khosrojerdi, M. Karami, Experimental investigation of graphene nanoplatelets nanofluid-based volumetric solar collector for domestic hot water systems, Sol. Energy 131 (Jun. 2016) 119–130.
[15] S. Iranmanesh, H. Chyuan Ong, B.C. Ang, E. Sadeghinezhad, A. Esmaeilzadeh, M. Mehrali, Thermal performance enhancement of an evacuated tube solar collector using graphene nanoplatelets nanofluid, J. Clean. Prod. 162 (2017) 121–129.
[16] R. Bubbico, G.P. Celata, F. D'Annibale, B. Mazzarotta, C. Menale, Experimental analysis of corrosion and erosion phenomena on metal surfaces by nanofluids, Chem. Eng. Res. Des. 104 (Dec. 2015) 605–614.
[17] A. Rashidi, et al., An investigation of electrochemical behavior of nanofluids containing MWCNT on the corrosion rate of carbon steel, Mater. Res. Bull. 48 (11) (Nov. 2013) 4438–4443.
[18] A.F. Ismail, A. Anuar, W. Rashmi, T. Yusaf, Corrosion effects of CNT-nanofluids on different metals, WIT Trans. Eng. Sci. (2014).
[19] K. Wu, H.-H. Ge, F. Wang, H.-W. Zhou, Corrosion behavior of brass in Tio2 nanofluids, IOP Conf. Ser. Mater. Sci. Eng. 230 (2017) 12011.
[20] Q. Yuan, et al., Influence of Al2O3 nanoparticles on the corrosion behavior of brass in simulated cooling water, J. Alloys Compd. 764 (Oct. 2018) 512–522.
[21] J.-Y. Sha, et al., Corrosion inhibition behaviour of sodium dodecyl benzene sulphonate for brass in an Al2O3 nanofluid and simulated cooling water, Corrosion Sci. 148 (Mar. 2019) 123–133.
[22] M. Baghalha, M. Kamal-Ahmadi, Copper corrosion in sodium dodecyl sulphate solutions and carbon nanotube nanofluids: a modified Koutecky-Levich equation to model the agitation effect, Corrosion Sci. 53 (12) (Dec. 2011) 4241–4247.
[23] D.F. Menicucci, A.R. Mahoney, Copper Corrosion and its Relationship to Solar Collectors:a Compendium, Jul. 2007. Albuquerque, NM, and Livermore, CA (United States).
[24] B. Cwalina, Biodeterioration of concrete, brick and other mineral-based building materials, in: Understanding Biocorrosion: Fundamentals and Applications, Elsevier Inc., 2014, pp. 281–312.
[25] F.C. Nagarajan, S.K. Kannaiyan, C. Boobalan, Intensification of heat transfer rate using alumina-silica nanocoolant, Int. J. Heat Mass Tran. 149 (Mar. 2020) 119127.
[26] P. Zhou, K. Ogle, The corrosion of copper and copper alloys, in: Encyclopedia of Interfacial Chemistry: Surface Science and Electrochemistry, Elsevier, 2018, pp. 478–489.
[27] T.E. Graedel, J.P. Franey, G.W. Kammlott, The corrosion of copper by atmospheric sulphurous gases, Corrosion Sci. 23 (11) (Jan. 1983) 1141–1152.
[28] B. Valdez Salas, et al., Copper corrosion by atmospheric pollutants in the electronics industry, ISRN Corros. 2013 (2013) 1–7.